Ion-channeling analysis of boron clusters in silicon

Selen, L. J. M.; Janssen, F. J. J.; van IJzendoorn, L. J.; de Voigt, M. J. A.; Theunissen, M. J. J.; Smulders, P. J. M.; Eijkemans, T. J.

Published in:
Journal of Applied Physics

DOI:
10.1063/1.1405838

Publication date:
2001

Ion-channeling analysis of boron clusters in silicon

L. J. M. Selen, F. J. J. Janssen, L. J. van IJzendoorn, M. J. A. de Voigt, M. J. J. Theunissen, P. J. M. Smulders, and T. J. Eijkemans

Citation: Journal of Applied Physics **90**, 4741 (2001); doi: 10.1063/1.1405838
View online: https://doi.org/10.1063/1.1405838
View Table of Contents: http://aip.scitation.org/toc/jap/90/9
Published by the American Institute of Physics

Ion-channeling analysis of boron clusters in silicon

L. J. M. Selen, F. J. J. Janssen, L. J. van IJzendoorn,[a] and M. J. A. de Voigt
Research Institutes CPS and COBRA, Cyclotron Laboratory, Department of Applied Physics, Eindhoven University of Technology, P.O. Box 513, 5600 MB Eindhoven, The Netherlands

M. J. J. Theunissen
Philips Research Laboratories, Eindhoven, The Netherlands

P. J. M. Smulders
Materials Science Center, University of Groningen, Groningen, The Netherlands

T. J. Eijkemans
Research School Cobra, Department of Applied Physics, Eindhoven University of Technology, Eindhoven, The Netherlands

(Received 6 November 2000; accepted for publication 30 July 2001)

We have measured axially channeled Rutherford backscattering spectra of $Si_{1-x}Ge_x$ nanofilms in silicon(001). A step in the yield of the host crystal was found for off-normal axes at the depth of the nanofilm. The step was measured as a function of the angle between the incoming beam and the [011] axis and shows two maxima. It is found that Monte Carlo simulations assuming tetragonal distortion reproduce the experimental results. A universal curve was derived which enables determination of the tetragonal distortion from ion-channeling experiments, for a given film thickness. The results are compared with XRD measurements. © *2001 American Institute of Physics.* [DOI: 10.1063/1.1405838]

I. INTRODUCTION

In modern semiconductor technology, films with a thickness in the nanometer regime (nanofilms) are of increasing importance. Particularly interesting are single-crystalline strained films, which are applied to semiconductor devices such as high-electron-mobility transistors, solid-state lasers, heterojunction bipolar transistors, and tunnel junctions. In strained films the lattice deformation is an important factor determining the band gap and the density of states (DOS), and thus the device properties. Characterization of the lattice deformation is, therefore, of vital importance and becomes an increasing challenge when the layer thickness decreases.

X-ray diffraction (XRD) is a well-known technique to investigate strain in thin films.[1–3] With high-resolution XRD it is possible to characterize depositions of less than 1 ML, when they are grown in a superlattice structure; i.e., to analyze a sub-ML-thickness film, 60 periods are needed.[4] However, the semiconductor devices mentioned above contain only one nanofilm.

Another well-known technique to investigate strain in thin films is MeV ion channeling. The tetragonal distortion can be measured by the shift of a so-called angular scan of the strained film with respect to the angular scan of the underlying host crystal along off-normal axes. Usually, this method is restricted to the analysis of thin films with a thickness typically larger than 20 nm, since a necessary condition for this procedure is a decrease of the scattering probability in the epitaxial film, for which a film thickness of at least 20 nm is required. When the epitaxial films are situated at the surface and are extremely thin (<10 nm), this can only be pursued by lowering the incident energy as demonstrated by the highly specialized medium-energy ion-scattering (MEIS) techniques.[5–8]

Ion beams with higher energies (2 MeV) are commonly available for standard Rutherford backscattering spectrometry (RBS) analysis, which allows us to measure samples with buried nanofilms. When in a buried commensurate nanofilm the length of the atomic strings is far below the typical lengths required to obtain an angular scan ($\geqslant 20$ nm for ion energies ≈ 2 MeV), the value of the strain can no longer be determined from the shift of the angular scan. In such a case, the shape of an angular scan and the angular position at which the minimum in the yield occurs are not representative for the nanofilm, and are primarily determined by the flux distribution (channeled or nonchanneled) emerging from the capping crystal reaching the nanofilm. Along the off-normal axes of the host crystal, the presence of such a film has the same effect as a stacking fault. Consequently, for channeling along off-normal axes, a sudden increase of the scattering yield can be measured. The strain in the thin film and its thickness determine the increase of the scattering yield. The magnitude of this step depends on the translation of the atomic strings with respect to the flux distribution emerging from the capping layer. Thus, this method basically provides a possibility to investigate nanofilms without looking at the atoms. With Monte Carlo simulations the increase in scattering yield can be related to the strain and thickness of the tetragonally deformed film.

[a]Author to whom correspondence should be addressed; present address: Cyclotron Laboratory, Department of Applied Physics, Eindhoven University of Technology, P.O. Box 513, 5600 MB Eindhoven, The Netherlands; electronic mail: L.J.van.IJzendoorn@tue.nl

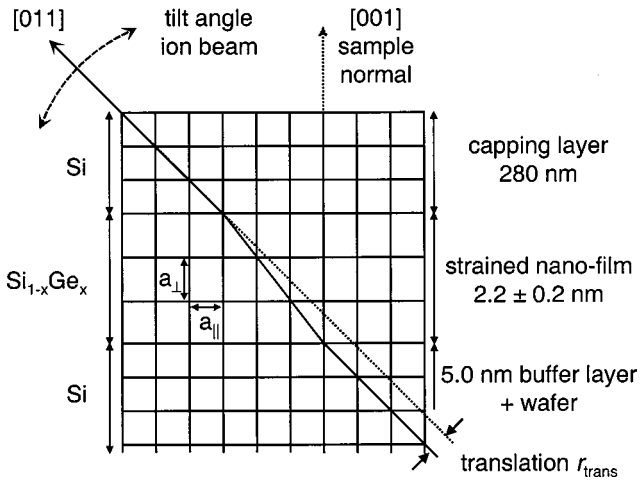

FIG. 1. Schematic drawing of the sample. The main crystal directions, the direction of the angular scans, the lattice constants, and the translation of the strings of the Si wafer are indicated.

Nowadays, single-crystalline layers with a thickness in the nm range can be accurately grown by atmospheric-pressure-chemical-vapor deposition (APCVD). Preliminary measurements on 2.2-nm-thick $Si_{1-x}Ge_x$ films in Si grown 280 nm below the surface demonstrated a relation between the translation of the host crystal and the magnitude of the increase of the scattering yield.[9] This article will describe the correlation between the translation of the host crystal caused by a strained nanofilm and the observed magnitude of the increase in the scattering yield for He^+ ions in the energy range of 2–3.5 MeV. Furthermore, XRD measurements and simulations on the same samples will be presented.

II. EXPERIMENT

Buried $Si_{1-x}Ge_x$ nanofilms in Si have been grown by APCVD on a 6 in. (001) oriented Si wafer at Philips Research Laboratories Eindhoven. At first the wafer was cleaned with H_2 at a temperature of 1100 °C, and then a 5.0 nm Si buffer layer was grown at 625 °C. Subsequently, a 2.2-nm-thick $Si_{1-x}Ge_x$ film was grown by deposition of GeH_4 and $SiCl_2$ at 625 °C. Finally, a 280 nm Si capping layer was deposited at 700 °C. Two different samples were prepared: the first and second samples contain $(4.6\pm0.3)\times10^{15}$ and $(6.4\pm0.3)\times10^{15}$ Ge/cm^2, respectively, as determined by 2 MeV Rutherford backscattering spectrometry analysis. The thickness of the $Si_{1-x}Ge_x$ films was measured by high-resolution transmission electron microscopy (HRTEM) to be (2.2 ± 0.2) nm for both samples. The Ge concentration of the samples amounts to (45 ± 5)% and (63 ± 6)%, respectively. In the remainder of this article these samples will be referred to as the 45% and 63% samples. A schematic drawing of the samples is shown in Fig. 1.

The tetragonal distortion is a quantity for the strain defined as $\varepsilon_T=\varepsilon_\perp-\varepsilon_\parallel=(a_\perp-a_\parallel)/a_V$, where $a_\perp$ is the perpendicular lattice constant, $a_\parallel$ the in-plane lattice constant, and a_V the Vegard crystal lattice constant for a bulk crystal with composition of the commensurate film. The in-plane strain $\varepsilon_\parallel$ and the perpendicular strain $\varepsilon_\perp$ are defined as the relative deviations of the lattice constants from the virtual crystal lattice constant. Since the critical layer thickness for Ge on Si is about 6 ML ($\approx$1.7 nm),[10] no dislocations are assumed to be present in the samples under investigation. This was verified with ion-channeling measurements along the [001] axis near the sample normal. The measurements pointed to the absence of dislocations near the nanofilm, which implies that the $Si_{1-x}Ge_x$ nanofilms are tetragonally deformed and that the $Si_{1-x}Ge_x$ unit cells are not relaxed to a cubic crystal lattice. The tetragonal distortion in the film amounts to $\varepsilon_T=0.033$ and 0.046 for the 45% and 63% samples, respectively. For a thickness of 2.2 nm, this leads to translations r_{trans} of the substrate $\langle011\rangle$ strings relative to those of the capping layer of 0.051 and 0.072 nm for the 45% and 63% samples, respectively (see Fig. 1).

The ion-channeling experiments have been performed with 2–3.5 MeV He^+ ion beams from the Philips AVF Cyclotron at Eindhoven University of Technology. The beam currents were between 5 and 30 nA. A rotating vane with a 88-nm-thick gold film is employed to measure the ion dose. The energy of He^+ ions scattered from the rotating vane is measured with a 25 mm^2 Canberra-passivated implanted planar silicon (PIPS) detector with an energy resolution of 15 keV.

For the ion-channeling experiments the samples were placed in a three-axes goniometer with an angular resolution $<0.005°$.[11] With two sets of slits the beam divergence was set to 0.07° full width at half maximum. Backscattered ions were detected with a 100 mm^2 Canberra PIPS detector with a resolution of approximately 17 keV, positioned at a backscattering angle of 130°. For axial channeling measurements a series of channeling spectra was obtained by varying the tilt angle ψ between the incoming beam and the [011] axis of the sample (see Fig. 1).

XRD measurements were performed with a Bede model 200 high-resolution (0.5 arc s) research diffractometer setup with a Bede channel cut collimator with a Si $\langle111\rangle$ reference crystal at the Eindhoven University of Technology. The $K\alpha_1$ x rays from a 2.2 kW Cu long fine focus source are detected with a NaI scintillation crystal and photomultiplier, which gives a dynamical range of 0.1–250 000 counts. In a $\theta,2\theta$ measurement the samples were investigated in grazing-incidence geometry on the {113} planes, with an incoming angle of 2.8°, the Bragg angle at 28.1°, and the detector at 56°.

III. CHANNELING

Figure 2 shows a typical RBS spectrum of the 63% sample with a step in the yield at the depth of the strained nanofilm. The spectrum is one of the spectra obtained in an angular scan through the [011] axis in the {001} plane. The sample was rotated over 0.16° from the [011] axis of the capping layer towards the [001] surface normal in the {100} plane. The step in the spectrum due to the presence of the strained nanofilm is magnified in Fig. 2(b). Since the stopping power for channeled ions depends on the detailed trajectories in the channels,[12] the exact depth in nm at which the nanofilm is situated cannot be determined easily from spectra

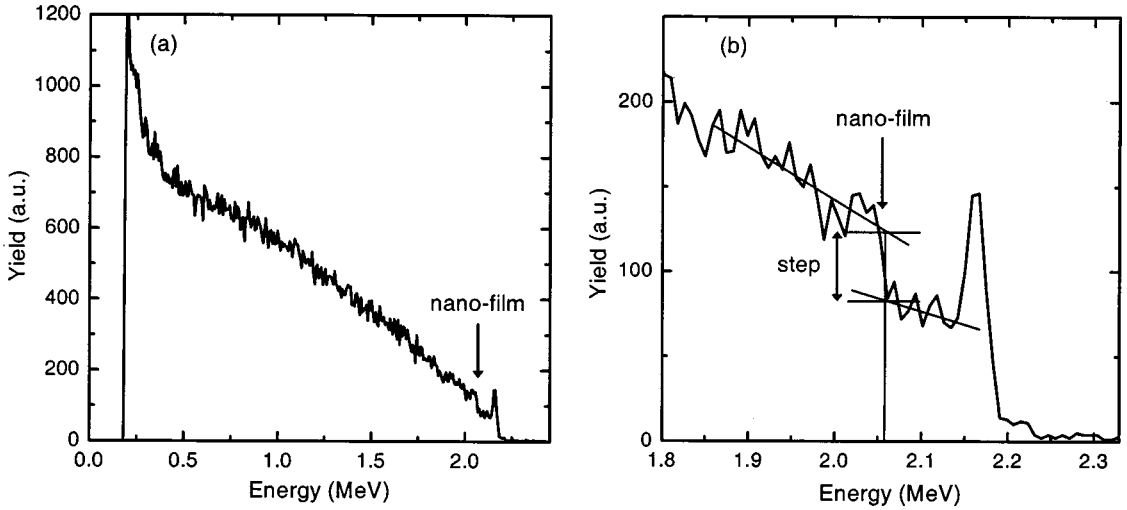

FIG. 2. RBS spectrum of the 63% sample tilted 0.16° away from the [011] axis of the Si capping layer using 3.5 MeV He^+ ions.

in channeling experiments. Monte Carlo simulations show that the stopping power experienced by the scattered ions giving rise to the step is within 10% of the value of the random stopping power.

The height of the step in the yield depends on the position of the atomic strings of the Si wafer relative to those of the capping layer. In Fig. 3 the height of the step in the spectrum is plotted as a function of the angle ψ for both samples. The experimentally found data points in Fig. 3 are taken from the channeled spectra after they have been normalized to the counts in the Au peak of the rotating vane and the step heights are normalized to the highest step in the angular scans. Figure 3 shows that for both the 45% and 63% samples, two maxima appear in the curve of the step height as a function of the angle ψ. It is remarkable that the angular separation between the two maxima $\psi_{\max}$, which is estimated with the guiding lines, is larger for the 45% sample, in which the atomic strings of the substrate are translated less. Furthermore, the curves are not completely symmetrical in ψ.

Similar experiments were performed with 2 MeV He^+ ions,[9] and also the angular separation $\psi_{\max}$ was larger for the 45% sample and the curves were not completely symmetrical in ψ. Table I shows the values of $\psi_{\max}$ for both samples and both energies. The values of $\psi_{\max}$ are larger for the measurements at 2 MeV. Note that the characteristic angle ψ_1,[13] which is a measure of the maximum incidence angle for ions to be captured in a channel and scales with the energy as $E^{-1/2}$, is larger at 2 than at 3.5 MeV. The ratios of $\psi_{\max}$ and ψ_1 are given in the fourth and fifth column of Table I, and within the uncertainty the measured $\psi_{\max}$ scales with ψ_1. In the next section, an analytical flux distribution model is used to explain qualitatively the observed channeling behavior.

IV. ANALYTICAL MODELING

Feldman and co-workers presented an analytical model which describes the dependence of the steady-state flux distribution within a channel on the angle ψ between the incoming beam and the crystal axis. Steady state means that the flux distribution does not change as a function of depth, which is expected at the depth of the nanofilms in the samples investigated.[12]

Under the assumption that the nanofilm does not influ-

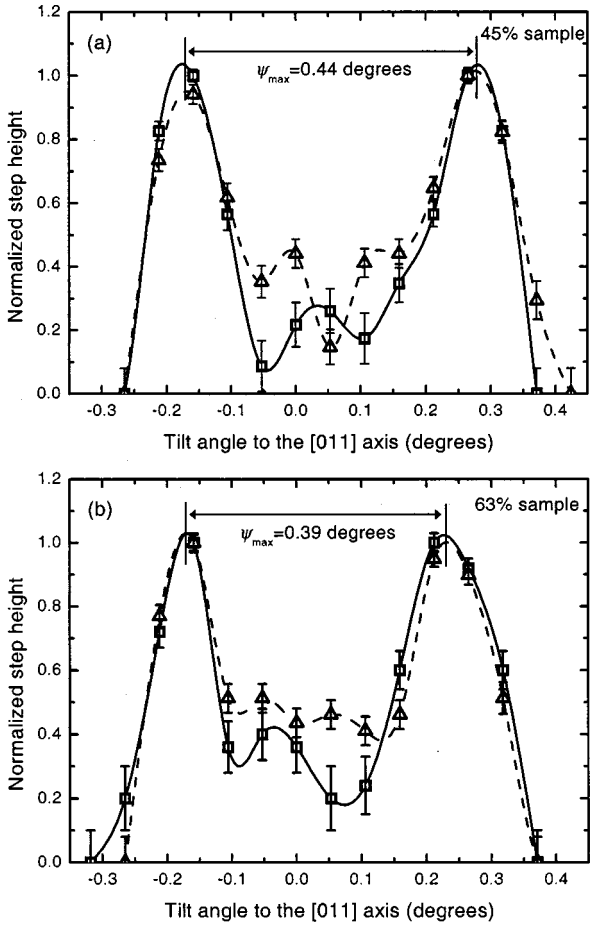

FIG. 3. Experimental normalized step height in the Si yield (squares) and calculated normalized step in the nuclear encounter probability (triangles) for 3.5 MeV He^+ ions for the 45% (a) and 63% (b) samples, as a function of the angle ψ between the [011] crystalline axis of the capping layer and the incoming beam. The guiding lines through the measured (solid line) and simulated data points (dotted line) are used to estimate the angular separation between the appearing maxima $\psi_{\max}$.

TABLE I. Values of ψ_{max} from ion-channeling experiments with 2 and 3.5 MeV He^+ ions, and these values scaled to the characteristic angle ψ_1.

	ψ_{max} (2 MeV)	ψ_{max} (3.5 MeV)	ψ_{max}/ψ_1 (2 MeV)	ψ_{max}/ψ_1 (3.5 MeV)
45% sample	(0.55±0.02)°	(0.44±0.02)°	0.94±0.03	0.99±0.03
63% sample	(0.49±0.02)°	(0.39±0.02)°	0.83±0.03	0.88±0.03
ψ_1	0.587°	0.444°		

ence the flux distribution emerging from the capping layer, the strings of the wafer will probe this flux distribution for off-normal axes at a certain distance r_{trans} from the atom rows of the capping layer. According to Lindhard's theory, ions with a certain transverse energy $E_\perp$ are distributed homogeneously within an equipotential contour given by $U_T = E_\perp$. The model is derived for a circular symmetric flux distribution around an atomic string, and for each angle ψ, the distance between the atomic row and the border of the equipotential contour with the highest flux is denoted by r_T.

Accordingly, the flux density takes its maximum at the position r_{trans} of the shifted strings if $r_{trans}=r_T$, and the corresponding angle $\psi=\psi_{Feld}$ yields the angular separation ψ_{max} according to the Feldman model, where $\psi_{Feld} = \psi_1\sqrt{\ln(r_0/r_T)}$ with r_0 the circular radius corresponding to the average area per channel. The values of ψ_{Feld} are given in Table II for both the samples and incoming He^+ ions at 2 and 3.5 MeV. In the last column ψ_{Feld} is compared to the experimentally found values of ψ_{max}, and apparently, a scaling factor is needed.

The angular dependence of the step height is explained qualitatively with this model, but for a steady-state flux distribution these are expected to be symmetric in ψ. The asymmetry and the structure in between the maxima show that the flux distribution is not steady state. A more detailed interpretation of the experiments can only be obtained with Monte Carlo simulations.

V. MONTE CARLO SIMULATIONS OF THE ANGULAR DEPENDENCE OF THE STEP HEIGHT

Monte Carlo (MC) channeling simulations have been performed with the program FLUX7, which is an improved and extended version of FLUX.[14] The calculations are based on binary collisions of the incoming ion and the target nuclei. In addition, the effect of distant rows of target atoms is accounted for by a continuum string potential. The thermal vibrations of the target atoms and the stopping of the projectile ions by target electrons in the solid are also incorporated. One of the output parameters of FLUX7 is the nuclear encounter probability (NEP) with a target atom to cause an event such as large-angle scattering (in RBS), a high-energy recoil of the target atom, or a nuclear reaction. The NEP is normalized to that of an equal number of randomly oriented trajectories through an equal distance within the lattice.

The FLUX7 simulation package is used to perform MC calculations of the NEP as a function of depth for the 45% and 63% samples. The strain in the $Si_{1-x}Ge_x$ film leads to a kink in the [011] channel, which can be simulated by rotating the velocity vector of the ions at the beginning and end of the $Si_{1-x}Ge_x$ film. Simulations were done for different translations (r_{trans}) of the atomic strings of the substrate. Since in FLUX7 the thickness of a layer can only be varied in discrete steps of 1 ML, a 8-ML-thick (2.3 nm) $Si_{1-x}Ge_x$ film is used in the calculations.

Figure 4 shows an example of the NEP as a function of depth. An increase in the NEP is found at the depth of the nanofilm, which corresponds to the step in scattering yield in the measured spectra. The step height in the NEP is calculated from the simulations and is plotted as a function of the angle ψ in Fig. 3. The angular separation of the two maxima in the simulated step height now agrees with the experimentally determined ψ_{max} for values of r_{trans} of $(5.3\pm0.5)\times10^{-2}$ and $(7.5\pm0.6)\times10^{-2}$ nm for the 45% and 63% samples, respectively. This corresponds to an 8-ML-thick nanofilm with (46±4)% Ge for the 45% sample and (65±5)% Ge for the 63% sample, resulting in a tetragonal distortion of 0.034±0.003 and 0.048±0.004, respectively. Note that contrary to the calculations with the Feldman model, no scaling factor is needed to explain the angular separation between the maxima.

The simulations show many detailed similarities with the experimental results: the separations between the appearing maxima in the step height are well within the error and the overall trends look very much alike. Furthermore, the angular dependence is not symmetric and this asymmetry agrees very well with that of the measurements. The asymmetry is attributed to the fact that the flux distribution does not reach steady state at the depth of the nanofilm. In addition, the Ge concentrations retrieved from the simulations are in good agreement with the values found from the combined RBS and HRTEM measurements.

Now, with FLUX7, we examine the assumption which was made before in Sec. I; i.e., the presence of the nanofilm can be considered as a stacking fault. FLUX7 allows us to

TABLE II. Values of ψ_{Feld} for 2 and 3.5 MeV He^+ ions and these values scaled to the experimentally found values.

	ψ_{Feld} (2 MeV)	ψ_{Feld} (3.5 MeV)	ψ_{Feld}/ψ_{max} (2 MeV)	ψ_{Feld}/ψ_{max} (3.5 MeV)
45% sample	1.36°	1.03°	2.47±0.07	2.34±0.08
63% sample	1.19°	0.90°	2.43±0.07	2.31±0.09

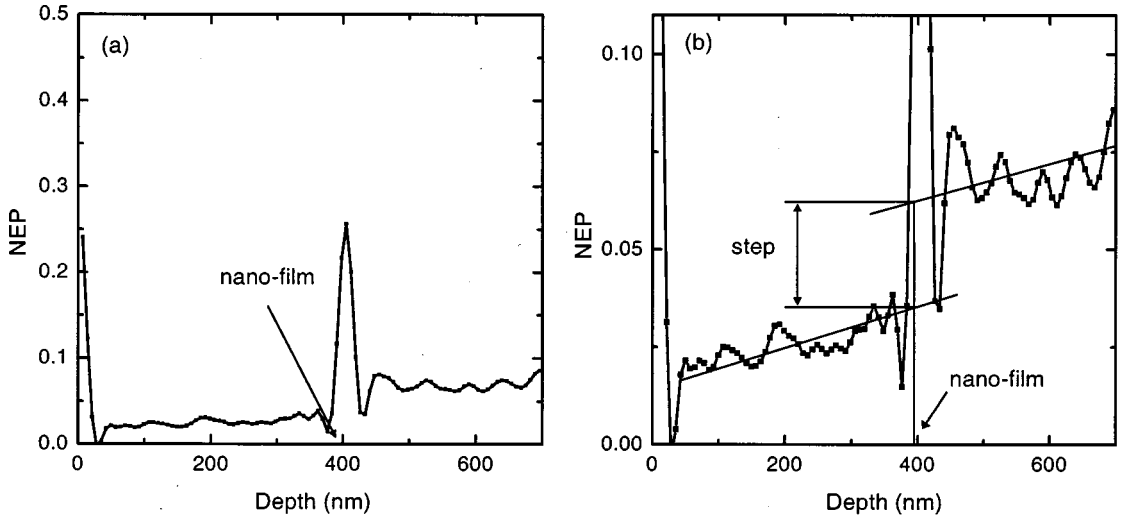

FIG. 4. Nuclear encounter probability (NEP) as a function of depth (a) and a magnification of the step in the NEP (b). The simulation is performed for the 63% sample tilted 0.21° away from the [011] axis using 3.5 MeV He^+ ions. The total NEP is plotted and, thus, for the nanofilm the NEP of Ge is added to the NEP of Si.

simulate a sample consisting of two silicon layers translated with respect to each other without the presence of the $Si_{1-x}Ge_x$ film. Simulations show that if for such a sample the translation is taken equal to the translation r_{trans}, which would be caused by the strained $Si_{1-x}Ge_x$ nanofilms, the curves of the step height as a function of ψ are identical for both samples within the statistical error. FLUX7 simulations thus support this assumption.

To investigate for which maximum thickness of the nanofilm this assumption, that the nanofilm does not influence the flux distribution, is still valid, simulations with combinations of tetragonal distortion and thickness were carried out. The combinations were chosen such that r_{trans} is the same for all cases. For layers thicker than $\approx$ 6 nm, the difference between $\psi_{\max}$ of these FLUX7 simulations and that of the experiments become larger than the errors (0.02°). This suggests that our method can be applied to strained films smaller than 6 nm.

VI. TETRAGONAL DISTORTION

In the previous section, we compared the ion-channeling measurements on the 45% and 63% samples with the FLUX7 simulations. More simulations are performed to relate the measured angular separation $\psi_{\max}$ to r_{trans} caused by the nanofilm. In these simulations the thickness of the nanofilm is kept constant at 2.3 nm, while r_{trans} is varied. This is done by varying the concentration of Ge in the $Si_{1-x}Ge_x$ nanofilm between 30% and 80%, which covers a wide range of physically interesting tetragonal distortions (0.022–0.059). To give the results a more universal character, $\psi_{\max}$ has been normalized to ψ_1, which is 0.587° in this case. Figure 5 shows the relation between the normalized $\psi_{\max}$ and the translation r_{trans}.

The graph in Fig. 5 is a universal curve that can be used to retrieve the tetragonal distortion from RBS ion-channeling measurements, when the thickness of the nanofilm has been determined with HRTEM. Notice that $\psi_{\max}$ seems to be a linear function of the tetragonal distortion for these combinations of thickness and tetragonal distortion, although the potential in the channel is not a linear function of the distance to the atomic rows.[12]

The error in the determination of the tetragonal distortion, resulting from the errors in the measured and the simulated $\psi_{\max}$, is on average $\pm$8%. In addition, the error of the thickness in the HRTEM measurement, which is $\pm$10% depending on the thickness of the film, must be taken into account.

VII. XRD

The samples have also been investigated with a Bede high-resolution XRD (HRXRD) facility at the Eindhoven University of Technology in order to investigate the consis-

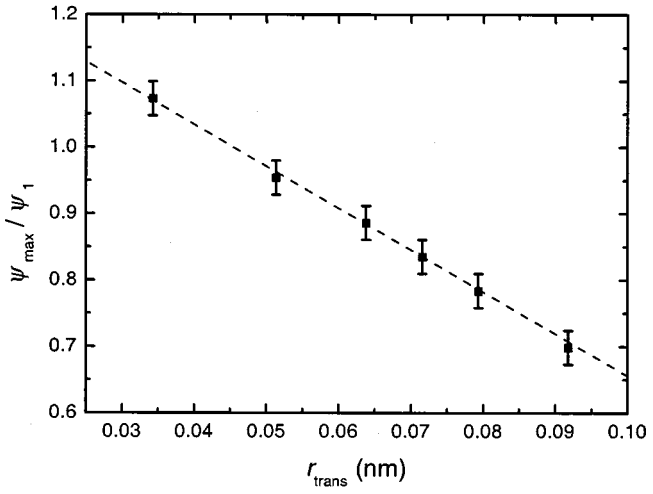

FIG. 5. Normalized angle $\psi_{\max}/\psi_1$ as a function of the translation r_{trans}. The points in the graph have been calculated with FLUX7 for 2 MeV He^+ ions and a silicon sample with a 2.3-nm-thick $Si_{1-x}Ge_x$ layer ($0.3 \leqslant x \leqslant 0.8$). The line is only to guide the eye.

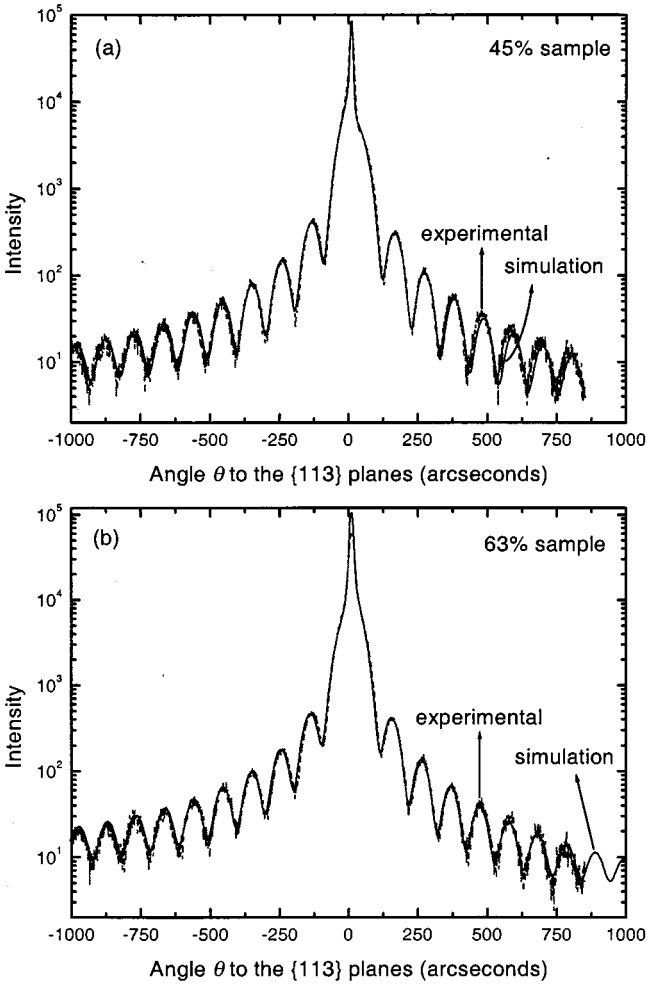

FIG. 6. Results of the grazing-incidence $\theta,2\theta$ scans of the {113} planes of the 45% (a) and 63% (b) samples, and the curves of the best fits from the RADS Mercury simulation program.

tency of the channeling results. A $\theta,2\theta$ scan of the {113} planes is made with a range of 2000 arc s for the incoming angle θ, and the grazing-incidence configuration is used, since it gives the best results. The resolution is 1 arc s and the measuring time per step is 2.5 s. The Bede RADS Mercury package, which is based on dynamical theory simulations, is used to analyze the XRD measurements.

Figure 6 shows the results of the measurements and the best fit from the simulations with RADS Mercury for the 45% and the 63% samples. The difference between the two measured curves is very small, but it can be seen that the pattern in the measured curves is translated a little to the left for the 63% sample, which can be expected when a higher compressive strain is present. Note that the parameter measured by XRD is the lattice spacing in the nanofilm. For the 45% sample, the best-fit through the measured curve is obtained for a thickness of (2.8 ± 0.1) nm and a Ge concentration of (43 ± 2)%. For the 63% sample, the best-fit parameters are a thickness of (2.7 ± 0.1) nm and a Ge concentration of (56 ± 2)%. The areal Ge density derived from the XRD measurements is $(5.6\pm0.5)\times10^{15}$ and $(6.9\pm0.5)\times10^{15}$ Ge/cm^2 for the 45% and 63% samples, respectively. Since the areal Ge density determined by RBS is considered to be more correct, we can conclude that the simulation of the XRD measurement on the 45% sample is not satisfactory. Furthermore, in both cases the thickness found in the XRD simulations is much larger than the value determined by HRTEM, (2.2 ± 0.2) nm.

A possible explanation might be tailing caused by Ge segregation during growth of the Si capping layer. Tailing caused by segregation is a phenomenon that is frequently encountered during nanofilm growth.[15–17] In the HRXRD simulations tailing can be incorporated by adding an extra layer of $Si_{1-x}Ge_x$ between the nanofilm and the capping layer, where the Ge concentration follows $\exp(-t/L)$ with t the distance to the capping layer/nanofilm interface and a constant $L=0.8$ nm as the decay length for the Ge concentration. Simulations have been performed incorporating the tailing, and the best-fit parameters of the areal Ge density, tetragonal distortion in the nanofilm, and t are given in Table III. It is interesting to note that now for both samples the total Ge areal density is in agreement with the values from the RBS measurements. For the 45% sample the value of the tetragonal distortion in the nanofilm derived from XRD agrees with that from ion channeling, but it does not for the 63% sample. However, the translation r_{trans} of the strings (which depends on both the tetragonal distortion and thickness) deduced from the XRD measurements on the 45% and 63% samples amounts to $(5.6\pm0.5)\times10^{-2}$ and $(7.3\pm0.6)\times10^{-2}$ nm, respectively, which agrees well with the ion-channeling results of $(5.3\pm0.5)\times10^{-2}$ and $(7.5\pm0.6)\times10^{-2}$ nm, respectively. The XRD measurements thus reveal tailing of Ge in the samples, which was not taken into account in the previous sections on ion channeling. The ion-channeling technique, however, only measures the translation r_{trans} for which tailing is not relevant.

VIII. CONCLUSIONS

We have applied the ion-channeling technique to samples with a (2.2 ± 0.2)-nm-thick buried tetragonally deformed $Si_{1-x}Ge_x$ nanofilm in Si. The spectra show a step in the yield of the host crystal. The angular dependence of the step height reveals two maxima indicative for the tetragonal distortion in the nanofilms. It appears that these experiments

TABLE III. Best-fit parameters from the RADS mercury simulations with an extra layer added to account for tailing of Ge atoms into the capping layer. Also, the resulting areal Ge density is given.

	Thickness nanofilm (nm)	Ge concentration nanofilm (%)	ϵ_T nanofilm	Thickness t tailing layer (nm)	Total areal density (10^{15} Ge/cm^2)
45% sample	2.2±0.1	44±2	0.032±0.002	0.8±0.2	5.1±0.5
63% sample	2.6±0.1	51±2	0.038±0.002	0.7±0.2	6.5±0.4

can be successfully simulated with Monte Carlo calculations. A universal curve is derived, which relates the tetragonal distortion with the measured angular separation of the maxima.

Investigation of the samples with HRXRD revealed tailing of Ge, and it can be concluded that a comprehensive view on the morphology of the nanofilm can only be obtained by a combination of the RBS ion-channeling method, HRXRD, and HRTEM.

ACKNOWLEDGMENTS

The authors wish to thank Paul Koenraad for his help with the interpretation of the XRD measurements and simulations.

[1] A. G. Dirks, P. H. L. Bancken, J. Politiek, N. E. B. Cowern, J. H. M. Snijders, J. G. M. van Berkum, and M. A. Verheijen, *Proceedings of Ion Implantation Technology '98*, edited by J. Matsuo, G. Takaoka, and J. Yamada (IEEE, Piscataway, NJ, 1999), Vol. 2, pp. 1167–1170.
[2] X. S. Wang, Y. J. Zhang, L. Y. Zhang, and X. Yao, Appl. Phys. A: Mater. Sci. Process. **68**, 547 (1999).
[3] S. Yamaguchi, M. Kariya, S. Nitta, T. Takeuchi, C. Wetzel, H. Amano, and I. Akasaki, J. Appl. Phys. **85**, 7682 (1999).
[4] L. Hart, M. R. Fahey, R. C. Newman, and P. F. Fewster, Appl. Phys. Lett. **62**, 2218 (1993).
[5] J. F. van der Veen, Surf. Sci. Rep. **5**, 199 (1985).
[6] J. Vrijmoeth, P. M. Zagwijn, J. W. M. Frenken, and J. F. van der Veen, Phys. Rev. Lett. **67**, 1134 (1991).
[7] A. Agarwal, H. J. Gossman, D. J. Eaglesham, D. C. Jacobson, T. E. Haynes, J. Jackson, Y. E. Erokhin, and J. M. Poate, *Proceedings of the 4th International Workshop on Measurement, Characterization and Modelling of Ultra-Shallow Doping Profiles in Semiconductors* [Appl. Mater. **49**, 1 (1997)].
[8] H. C. Lu, E. P. Gusev, E. Garfunkel, and T. Gustafsson, Surf. Sci. **351**, 111 (1998).
[9] L. J. M. Selen, F. J. J. Janssen, L. J. van IJzendoorn, M. J. J. Theuniseen, P. J. M. Smulders, and M. J. A. de Voigt, Nucl. Instrum. Methods Phys. Res. B **161-163**, 492 (2000).
[10] L. C. Feldman, J. Bevk, B. A. Davidson, H.-J. Gossmann, and J. P. Mannaerts, Phys. Rev. Lett. **59**, 664 (1987).
[11] P. W. L. Van Dijk, Ph.D. thesis, Eindhoven University of Technology (1997).
[12] L. C. Feldman, J. W. Mayer, and S. T. Picraux, *Materials Analysis by Ion Channeling* (Academic, New York, 1982).
[13] M. Grundmann, O. Stier, and D. Bimberg, Phys. Rev. B **52**, 11 969 (1995).
[14] P. J. M. Smulders and D. O. Boerma, Nucl. Instrum. Methods Phys. Res. B **29**, 471 (1987).
[15] P. C. Zalm, C. J. Vriezema, D. J. Gravesteijn, G. F. A. van de Walle, and W. B. de Boer, Surf. Interface Anal. **17**, 556 (1991).
[16] P. C. Zalm, G. F. A. van de Walle, D. J. Gravesteijn, and A. A. van Gorkum, Appl. Phys. Lett. **55**, 2520 (1989).
[17] D. J. Gravesteijn, P. C. Zalm, G. F. A. van de Walle, C. J. Vriezema, A. A. van Gorkum, and L. J. van IJzendoorn, Thin Solid Films **183**, 191 (1989).